ARTICLE

Check for updates

Periodic island-layer-island growth during deposition of ultrastable metallic glasses

Fan Yang[1,2], Chao Wang[1], Haiyang Bai[1,3,4], Weihua Wang[1,3,4] & Yanhui Liu [1,3,4 ✉]

The fast exploration of low energy configuration by surface atoms is believed to favor the formation of ultrastable metallic glasses, prepared by physical vapor deposition. Here, we find that the rearrangement of surface atoms is collective, rather than being dominated by individual atoms. Specifically, we experimentally observe the growth process of ultrastable metallic glasses at monolayer resolution, which follows a periodic island-layer-island pattern with morphology variation between islands and flat surfaces. The estimated surface diffusion coefficient is orders of magnitude higher than that for bulk diffusion. The fast surface dynamics allow the newly deposited clusters on the flat surface to form local islands with spherical shape, which substantially reduces the surface free energy in each island-layer-island growth cycle. Our findings are helpful for understanding the growth mechanisms of ultrastable metallic glasses and potentially for tailoring their properties.

[1] Institute of Physics, Chinese Academy of Sciences, Beijing, China. [2] School of Physical Science, University of Chinese Academy of Sciences, Beijing, China. [3] Center of Materials Science and Optoelectronics Engineering, University of Chinese Academy of Sciences, Beijing, China. [4] Songshan Lake Materials Laboratory, Dongguan, Guangdong, China. ✉email: yanhui.liu@iphy.ac.cn

Ultrastable glasses have attracted increasing attention for their substantially enhanced thermodynamic and kinetic stability[1–5] as well as the associated exceptional mechanical properties[3,6]. Such enhanced stability and mechanical properties are important for their technological applications in broad areas such as coating materials, electronic and magnetic devices, amorphous pharmaceuticals, etc[1,4,7]. From the fundamental perspective, the extremely low energy of ultrastable glasses approaching the ground state and near-equilibrium configuration suggests that they bear meaningful information for the understanding of ideal glass, which may open a new avenue to unveil the nature of glass and glass transition[1,2,8–10].

Usually, ultrastable glasses are achieved by physical vapor deposition at a low deposition rate on a substrate heated to a high temperature ranging from $0.65T_g$ to $0.85T_g$, where T_g is the glass transition temperature[1,3,7,11]. The formation of ultrastable glasses has been primarily ascribed to the fast rearrangement of surface atoms to a low energy configuration due to the enhanced mobility of the liquid-like surface layer at high substrate temperature along with the sufficient time at a low deposition rate for such atomic rearrangement[1–3,12]. Based on the phenomenon that decreasing deposition rate can significantly enhance the stability of glasses[2,8], our recent study indicates that deposition rate has an essential role for the system to reach ultrastable states and the heated substrate is not a prerequisite for the fabrication of vapor-deposited ultrastable metallic glasses (UMGs)[4]. This implies that the formation process has a great impact on the characteristics of the obtained glasses. Therefore, unveiling the microstructural process leading to the formation of ultrastable glasses is essential for tailoring their properties and exploring the origin of their stability. Nonetheless, a detailed understanding of the growth dynamics of ultrastable glasses and the structural origin leading to their stability is still lacking. It remains unknown how the atomic rearrangement proceeds and how the competition of thermodynamics and kinetics ensure the lower energy and ultrastable state.

In this work, we report the observations on the growth process of UMGs by recording the evolution of surface morphology with deposition time. We found that the growth of UMGs follows a periodically repeated island-layer-island pattern. The surface morphology cyclically varies between isolated islands and flat surfaces. In each cycle, the newly deposited materials reach a low energy state by collective rearrangement that leads to the formation and coalescence of the local spherical surface due to the high atomic mobility and low deposition rate. Our findings provide a new understanding of the growth of UMGs and bear important insight into the phenomena happening in UMGs.

Results

Experiment. Following our previous protocol[4], we prepared the UMGs by using ion beam assisted deposition (IBAD) at room temperature, as schematically illustrated in Supplementary Figure 1. The surface morphologies were observed by atomic force microscope (AFM) after the deposition process. The time from the end of deposition to AFM scan is <5 minutes. To confirm the reproducibility of the experimental results, at least three samples were prepared under each growth condition, and AFM scanning was carried out at more than three different locations for each sample. Details about the sample preparation and AFM measurement can be found in the Method section. Microstructural characterizations by X-ray diffraction analysis and transmission electron microscopy confirmed the fully amorphous structures of the deposited films (Supplementary Figure 2).

Periodic island-layer-island growth. Figure 1 shows the evolution of surface morphology as a function of deposition time for $Zr_{46}Cu_{46}Al_8$ film grown on Si_3N_4 substrate, except for deposition time, all other deposition conditions are maintained the same for each film. The deposition rate used for the film is 1.07 nm min^{-1}, which is low enough to obtain UMG[4]. By considering the weighted average diameters of the constituent elements and deposition rate, the time required to grow a monolayer is estimated to be 16 s, which is comparable to the time interval of 15 s between each successive image. Therefore, these images, showing nearly monolayer-by-monolayer evolution of surface morphology, provide a meaningful resolution to capture the detailed characteristics associated with UMG growth.

As shown in Fig. 1a–c, the initial growth stage of UMG is featured by smoothening the height fluctuation on the substrate surface (see the images from 0 to 30 s). After that, the growth (from 45 s to 90 s) experiences a process similar to the early stage of Volmer–Weber growth mode for crystalline materials[13,14], i.e., island formation followed by island coalescence and percolation (Fig. 1d–g). During this process, the isolated islands grow with increasing deposition time in both size and number density, until they are in contact with each other and coalesce to form new islands with the larger sizes. The new islands continue to grow in the manner of their predecessors, but the time for further coalescence becomes longer due to the larger size. Elongated worm-like islands are created when island contact occurs but coalescence is incomplete (Fig. 1d). With increasing deposition time, the elongated islands continue to grow in size and connect to each other (Fig. 1e), leading to the formation of the percolating structure (Fig. 1f). Further deposition finally leads to the formation of a continuous and flat film (Fig. 1g).

In contrast to the Volmer–Weber growth mode, however, the film does not maintain the flat surface with increasing deposition time. Instead, uneven structure re-appears on the surface (Fig. 1h, 105 s), which is characterized by a surface morphology covered with isolated droplet-like islands and some newly formed elongated islands (Fig. 1i). This morphology is nearly the same as that at a growth time of 45 s (Fig. 1d). Then, both worm-like structures and percolating structures gradually form (Fig. 1j), followed by the formation of a flat surface (Fig. 1k). With increasing deposition time, the surface morphology of the growing film periodically repeats such a process. For example, the formation of isolated islands and their coalescence emerges again from 165 s to 180 s (Fig. 1l–m). Subsequently, they evolve to the worm-like islands at 195 s (Fig. 1n), and then to a continuous flat surface at 210 s (Fig. 1o). At 225 s, an uneven structure re-emerges again and the new cycles begin (see Fig. 1p–x). The evolution of surface morphology within one growth cycle can also be vividly reflected by the line profiles (Supplementary Figure 3a).

The topography evolution leads to obvious periodic variation in surface roughness. As shown in Fig. 2, with increasing deposition time, the surface roughness exhibits obvious fluctuation in a nearly periodic pattern, which is distinctly different from traditional film growth modes, such as layer growth, island growth, or layer-plus-island growth[15]. The periodic cycle is characterized by the topography variation from nearly atomically flatness to a rougher surface due to the repeated occurrence of islands formation and coalescence. According to the roughness variation, the period between two flat surfaces is estimated to be 60 s.

We further carried out observations at a much longer deposition time, i.e., 3600–3675 s (Fig. 2b and Supplementary Figure 4). The evolution of surface morphology is the same as that at a shorter deposition time. Furthermore, the periodical island-layer-island growth persists while using Al_2O_3 as substrate (Supplementary Figure 5). The deposition of the $Cu_{50}Zr_{50}$ (see Fig. 2c and Supplementary Figure 6) and $Fe_{73}Si_7B_{17}Nb_3$ (see Supplementary Figure 7 and Supplementary Figure 8) UMGs

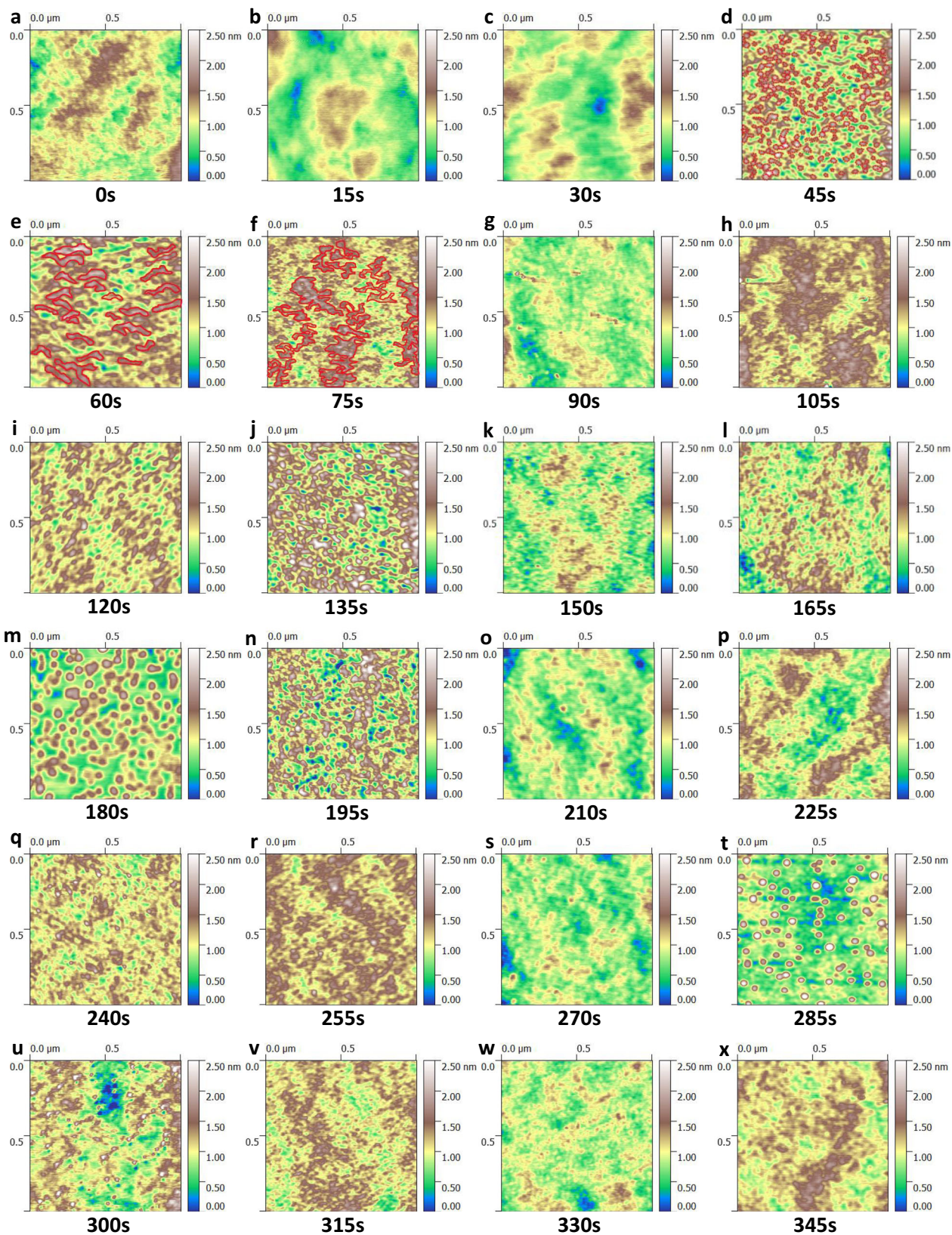**Fig. 1 Surface morphology evolution of Zr$_{46}$Cu$_{46}$Al$_8$ UMG. a–x** show the AFM images taken at different deposition times. The time interval for the images is 15 s, and the UMG was deposited at room temperature (~0.43T_g) with a deposition rate of 1.07 nm min^{-1}. The UMG was deposited on Si$_3$N$_4$ substrate. The red lines in **d–f** indicate the profiles of the islands on the surface. The lateral size of the images is 1 µm.
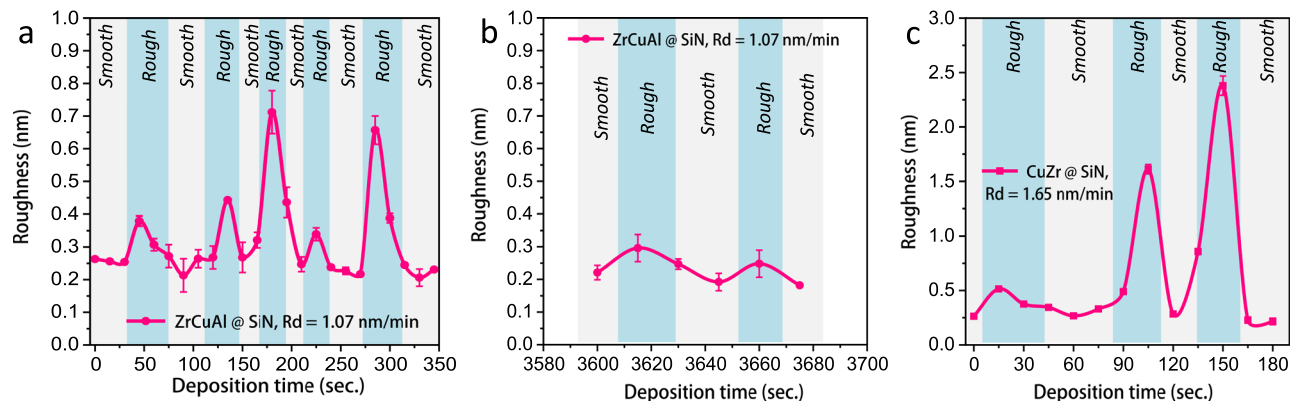
Fig. 2 Variation in surface roughness of UMG. The variation of surface roughness as a function of deposition time for $Zr_{46}Cu_{46}Al_8$ films deposited on Si_3N_4 substrate at a deposition rate of 1.07 nm min⁻¹. **a** The roughness change in the initial stage of deposition. **b** The roughness change at longer deposition time. **c** $Cu_{50}Zr_{50}$ films deposited on Si_3N_4 substrate at a deposition rate of 1.65 nm min⁻¹ over time from 0 s to 180 s. The error bars indicate the standard deviation from five measurements.
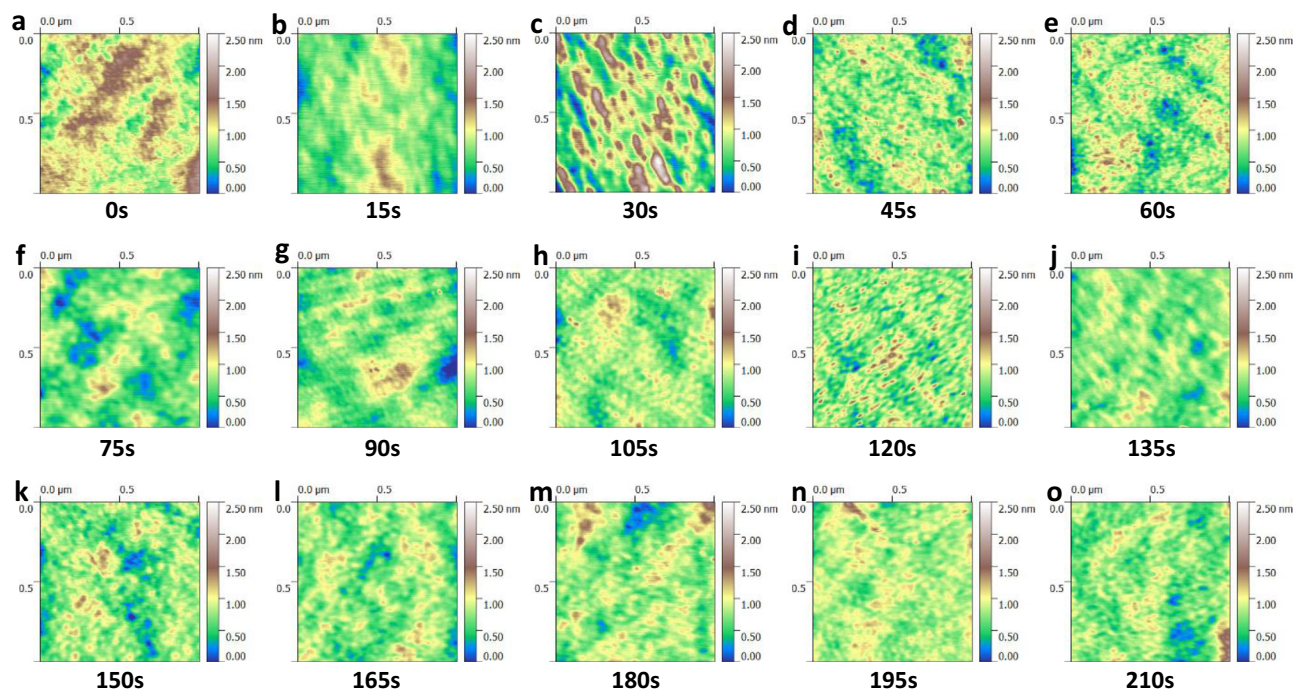

Fig. 3 Surface morphology evolution of MG with higher deposition rate. a–o are AFM images showing the surface morphology at different times. The time interval for the images is 15 s. The $Zr_{46}Cu_{46}Al_8$ films deposited with a rate of 4.16 nm min⁻¹ at room temperature on the Si_3N_4 substrate. The lateral size of the image is 1 μm.

verifies that the periodic island-layer-island growth is independent of specific alloy composition.

However, the periodic growth pattern is absent at a higher deposition rate. Figure 3 shows the surface morphology of $Zr_{46}Cu_{46}Al_8$ film grown on Si_3N_4 substrate at a deposition rate of 4.16 nm min⁻¹, which is incapable to achieve UMG[4]. Initially, smoothening of the height fluctuation on the substrate surface due to the accumulation of incoming atoms can be seen (Fig. 3b). In distinct contrast to the case at a lower deposition rate, island formation occurs only in the initial stage of film growth (Fig. 3c). Once the continuous film is formed, the surface topography does not change with deposition time and the recurrence of isolated islands cannot be observed (Fig. 3d–o). As shown in Fig. 4a, after the formation of the flat surface (at the growth time of 45 s), the roughness remains a constant of ~0.2 nm. This suggests that the morphologies are

probably produced by the random accumulation of incoming atoms with increasing deposition time, which is consistent with the previous report[11,15,16].

In order to confirm the absence of island formation at a high deposition rate, we reduce the time interval between each successive image to 5 s, which is close to the time required for the growth of monolayer at the deposition rate of 4.16 nm min⁻¹. Again, the surface topography remains essentially the same with increasing deposition time (see Supplementary Figure 9). The periodic island-layer-island cycle cannot be seen, and the surface roughness with prolonged deposition time remains constant (Fig. 4b). The line profiles also reveal the invariant surface morphology (Supplementary Figure 3c). We further confirmed that the island-layer-island growth is absent for $Cu_{50}Zr_{50}$ film at a high deposition rate (Supplementary Figure 10 and Supplementary Figure 11). Therefore, the occurrence of island-layer-island
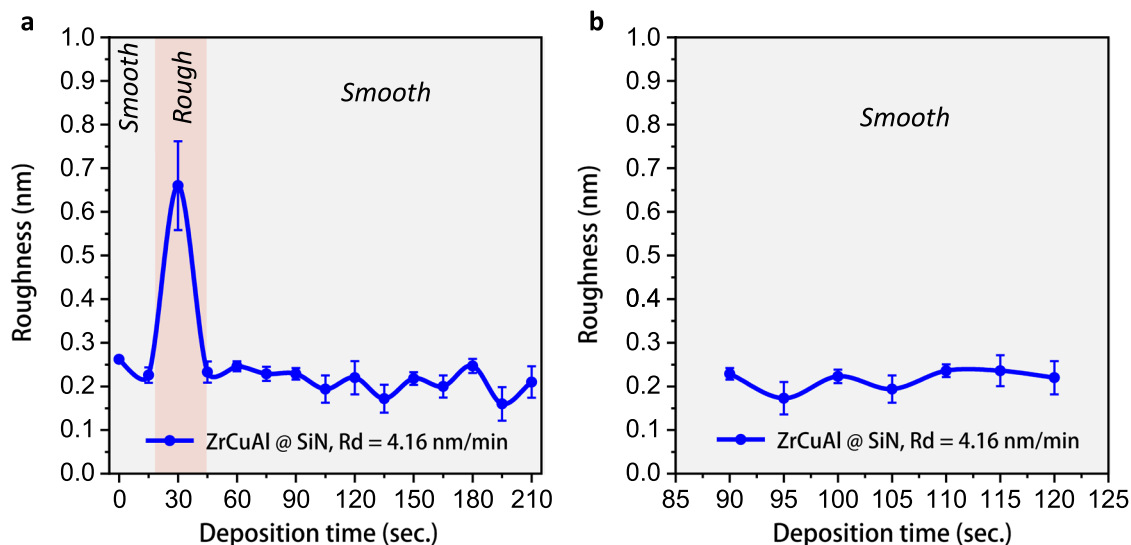
Fig. 4 Variation in surface roughness of MG with higher deposition rate. The $Zr_{46}Cu_{46}Al_8$ films were deposited at a rate of 4.16 nm min^{-1} on Si_3N_4 substrate. **a** The time interval between the data points is 15 s. **b** The time interval between the data points is 5 s. The error bars indicate the standard deviation of five measurements.

growth is dependent on the deposition rate, and the formation of UMGs is associated with the unique island-layer-island growth.

Competition between thermodynamic and kinetic. We next elaborate on why the films were grown at a lower deposition rate exhibit the periodic growth pattern. From the thermodynamic point of view, the incoming atoms generally first form cluster-like islands on the substrate followed by coalescence to reduce the surface-free energy[17], as $r_1{}^2 + r_2{}^2 \geq r_3{}^2$ when $r_1{}^3 + r_2{}^3 = r_3{}^3$, where r_1 and r_2 are the radius of the isolated islands and r_3 is the radius of the merged island. The surface energy can be calculated by $G = \gamma A$, where γ is the specific surface-free energy and A is the surface area of the island[17]. This is the ordinary island growth of crystal films, by which the islands finally form a continuous flat surface[13,17]. Previous investigations indicate that the surface of glasses and metallic glass nanoparticles exhibits liquid-like behavior and the dynamics of the surface and nanoparticles is orders of magnitude faster compared with that of the bulk[2,18–23]. Both the continuous flat film surface and the newly deposited clusters can thus be assumed as objects covered with viscous liquid of fast dynamics and high mobility. Upon the arrival of the newly deposited viscous clusters onto the viscous film surface, the clusters have the tendency to form a local spherical surface to reduce the free energy of the entire surface, because the viscosity is not low enough for the clusters to immediately blend into the film surface. At low deposition rate, the newly deposited clusters arriving at the continuous flat surface gain sufficient time to rearrange themselves to form spherical islands and coalesce due to their liquid-like mobility. However, the mobility of the clusters decreases with increasing size. When the size of the islands reaches a critical value (~9 nm, see Table 1), the time window to grow a monolayer (~16 s) is not enough for the coalescence to complete. With the incoming of more atoms, the islands become in connection and form elongated and percolation structures, which finally results in a flat surface. As schematically illustrated in Fig. 5, the characteristic that distinguishes the observed growth process in UMGs from other growth modes is the repeated formation of islands on a flat film surface. Hence, there exists a competition between thermodynamic driving forces to reduce surface-free energy and kinetic constraint associated with the time window for the formation and coalescence of the local

Table 1 Calculation of surface diffusion coefficient.

Alloy	Growth time (s)	t_c (s)	R_c (nm)	D_S (nm^2 s^{-1})
$Zr_{46}Cu_{46}Al_8$	45	15	8.8	0.58
	120	30	10.0	0.48
	195	45	10.9	0.46
	240	30	9.8	0.45
	300	30	9.4	0.38
	3615	15	8.2	0.44
$Cu_{50}Zr_{50}$	30	30	13.7	2.35
	90	30	15.1	3.46
	135	15	12.0	2.76

The parameters for the calculation of surface diffusion coefficient, D_S, include the critical island size R_c and the critical growth time t_c at which the surface evolves from a flat to a worm-like morphology. The $Zr_{46}Cu_{46}Al_8$ and $Cu_{50}Zr_{50}$ films were grown on Si_3N_4 substrate.

spherical surface during the deposition process. When the thermodynamic factors are dominant, the periodic island-layer-island growth might contribute to the lower energy state of UMG by minimization of surface-free energy in each cycle.

Surface diffusion coefficient. The fast surface dynamics and high mobility, which play a vital role in the periodic island-layer-island growth, is confirmed by the surface diffusion coefficient estimated with the observed surface morphologies. According to the "kinetic freezing model", the surface diffusion coefficient, D_S, can be estimated via $D_s = \frac{kTR_c{}^4}{t_c\gamma\Omega^{4/3}}$, where k is Boltzmann constant, T is deposition temperature, γ is the specific surface-free energy (1.36 J m^{-2} for $Zr_{46}Cu_{46}Al_8$[24] and 1 J m^{-2} for $Cu_{50}Zr_{50}$[25]), and $\Omega = \frac{M}{N_A \times \rho}$ is the volume of the component (M is the molar mass, N_A is Avogadro constant, the density ρ is 7.021 g cm^{-3} for $Zr_{46}Cu_{46}Al_8$[26] and 7.4 g cm^{-3} for $Cu_{50}Zr_{50}$[27]. In the equation, R_c and t_c is the critical island size and the corresponding growth time when the surface topography changes from isolated spherical islands to the worm-like elongated islands[14,28]. For each cycle of the island-layer-island growth, R_c and t_c can be obtained from the surface topography and the corresponding deposition time. The estimated D_S and the parameters used for each cycle are summarized in Table 1. On average, the $Zr_{46}Cu_{46}Al_8$ film exhibits a
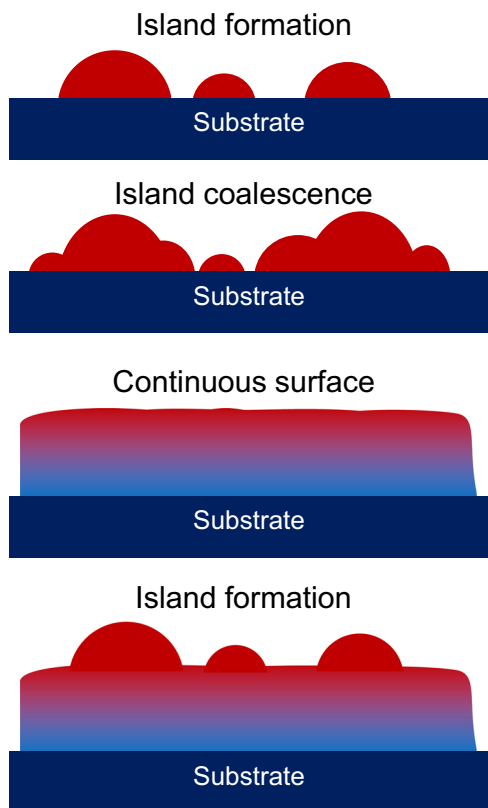
Fig. 5 Island-layer-island growth. The schematic diagram showing the island-layer-island growth of UMGs.

D_S of ~0.47 nm² s⁻¹ for a short deposition time. The value is 6~8 orders of magnitude higher than that of the bulk diffusion coefficient D_B at the same temperature ($D_{B\_Zr} = 2.95 \times 10^{-9}$ nm² s⁻¹, $D_{B\_Cu} = 9.07 \times 10^{-7}$ nm² s⁻¹, $D_{B\_Al} = 8.89 \times 10^{-7}$ nm² s⁻¹)[29], consistent with the observations of fast surface diffusion in other amorphous materials[18,30–34]. As shown in Table 1, $Cu_{50}Zr_{50}$ UMG also exhibits a high D_S of 2.86 nm² s⁻¹ on average, which is five orders of magnitude higher than the bulk diffusion coefficient of $Cu_{50}Zr_{50}$ at the same temperature[35]. A similar estimation for long deposition time (e.g., >3600 s) yields D_S of 0.44 nm² s⁻¹ for $Zr_{46}Cu_{46}Al_8$. The orders of magnitude higher surface diffusion coefficient than the bulk diffusion coefficient indicates that the surface of metallic glass film exhibit significantly faster dynamics. The nearly identical D_S at short and long deposition times confirms the persistence of the periodic island-layer-island growth throughout the growth of UMG.

Discussion

The origin for the formation of UMG by physical vapor deposition has been ascribed to the fast surface dynamics coupled with a low deposition rate, which results in prolonged relaxation time and increased mean free path of the surface atoms and allows the surface atoms to explore stable local configurations of lower energy state[1,3,4,7]. However, our results indicate that the growth of UMG is a result of repeated formation and coalescence of spherical islands after the occurrence of a flat surface. The rearrangement of surface atoms is actually a cooperative and collective behavior, instead of the exploration of local configurations by individual atoms. With a low deposition rate, the clusters gain sufficient time to rearrange into spherical topography and coalesce collectively in each layer to minimize surface-free energy of the layer.

Recently, it has been found that upon annealing UMG exhibits accelerated dynamics towards shorter time scales, which is opposite to the behavior of conventional MG. Such a phenomenon, called anti-aging, indicates that pre-annealing can significantly reduce the structural relaxation times of UMGs[36]. The observed island-layer-island growth provides a possible structural explanation for anti-aging. In ultrastable polymer glass, the microstructure was found to be anisotropic, because the orientation of the molecules can be trapped in the two-dimensional film surface during deposition[37]. Despite that the molecular orientation is absent in MG, the periodic island-layer-island growth can result in structural modulation along the growth direction in the deposited UMG. For example, the development of medium-range orders and chemical ordering are constrained in 2D, resulting in incomplete local ordering along the direction of film growth. To eliminate the structural modulation, annealing is required and the time is much longer than that for structural relaxation[37], leading to apparently long relaxation time for as-deposited UMGs[36]. Once the structural modulation is removed after pre-annealing, the UMGs behave in the similar way as conventional MGs.

Conclusion

In summary, we found that the UMGs prepared by PVD exhibit a unique island-layer-island growth process by which the surface morphology varies periodically between the isolated islands and flat surface. Under the combined effect of the fast surface dynamics and the wide time window, the clusters deposited at low deposition rate gain sufficient time to form spherical islands and coalesce to minimize the surface-free energy in each growth cycle. The rearrangement of surface atoms happened during the growth of UMGs is cooperative and collective. Such growth process may contribute to the low energy state and high stability of UMGs. Our findings may shed new light on the understanding of UMGs and tuning their properties by control the growth conditions.

Methods

Metallic glass films prepared by IBAD. The base pressure was better than 4×10^{-4} Pa, and the working argon pressure was maintained at 2.5×10^{-2} Pa. $Zr_{46}Cu_{46}Al_8$ and $Cu_{50}Zr_{50}$ metallic glasses were selected as model systems. Two types of substrates were used. One is Si wafer covered with an 80-nm-thick Si_3N_4 layer, and the other is Al_2O_3. To remove any possible impurities or contaminants on the surfaces, pre-sputtering was carried out on the targets with a beam energy of 750 eV and an ion beam current of 35 mA for >200 s. The substrates were cleaned by using ion beam with an energy of 550 eV and a current of 30 mA for 120 s. Deposition was conducted with a beam energy of 750 eV. The deposition rates were controlled by tuning the beam current from 5 mA to 30 mA. Film thickness was measured by using X-ray reflection technique. The deposition rates were estimated from the measured film thickness (Supplementary Figure 12) and deposition time, as shown in Supplementary Table 1.

Atomic force microscope analysis. The surface morphologies were observed by using an MFP-3D-SA standard AFM under AC Mode. Tap 300 Al-G probe with a resonant frequency of 300 kHz and a force constant of 40 N m⁻¹ was used in AFM characterizations. Each AFM scan took about three minutes. During the scanning process, the phase was always <90° while the trace and retrace curves corresponding to the obtained topography were almost identical, proving the high accuracy of the scanning results.

Data availability

The authors declare that the data supporting the findings of this study are included within the paper and available from the corresponding author on reasonable request.

References

1. Swallen, S. F. et al. Organic glasses with exceptional thermodynamic and kinetic stability. *Science* **315**, 353–356 (2007).

2. Singh, S., Ediger, M. D. & de Pablo, J. J. Ultrastable glasses from in silico vapour deposition. *Nat. Mater.* **12**, 139–144 (2013).
3. Yu, H. B., Luo, Y. S. & Samwer, K. Ultrastable metallic glass. *Adv. Mater.* **25**, 5904–5908 (2013).
4. Luo, P. et al. Ultrastable metallic glasses formed on cold substrates. *Nat. Commun.* **9**, 1389 (2018).
5. Yu, H. B., Tylinski, M., Guiseppi-Elie, A., Ediger, M. D. & Richert, R. Suppression of beta relaxation in vapor-deposited ultrastable glasses. *Phys. Rev. Lett.* **115**, 185501 (2015).
6. Kearns, K. L., Still, T., Fytas, G. & Ediger, M. D. High-modulus organic glasses prepared by physical vapor deposition. *Adv. Mater.* **22**, 39–42 (2010).
7. Zhang, K. et al. Ultrastable amorphous Sb_2Se_3 film. *J. Phys. Chem. B* **121**, 8188–8194 (2017).
8. Kearns, K. L. et al. Hiking down the energy landscape: progress toward the Kauzmann temperature via vapor deposition. *J. Phys. Chem. B* **112**, 4934–4942 (2008).
9. Ediger, M. D. Perspective: highly stable vapor-deposited glasses. *J. Chem. Phys.* **147**, 210901 (2017).
10. Dawson, K. J., Kearns, K. L., Yu, L., Steffen, W. & Ediger, M. D. Physical vapor deposition as a route to hidden amorphous states. *Proc. Natl Acad. Sci. USA* **106**, 15165–15170 (2009).
11. Kearns, K. L., Swallen, S. F., Ediger, M. D., Wu, T. & Yu, L. Influence of substrate temperature on the stability of glasses prepared by vapor deposition. *J. Chem. Phys.* **127**, 154702 (2007).
12. Reid, D. R., Lyubimov, I., Ediger, M. D. & de Pablo, J. J. Age and structure of a model vapour-deposited glass. *Nat. Commun.* **7**, 13062 (2016).
13. Yu, X., Duxbury, P. M., Jeffers, G. & Dubson, M. A. Coalescence and percolation in thin metal-films. *Phys. Rev. B* **44**, 13163–13166 (1991).
14. Ruffino, F. & Grimaldi, M. G. Island-to-percolation transition during the room-temperature growth of sputtered nanoscale Pd films on hexagonal SiC. *J. Appl. Phys.* **107**, 074301 (2010).
15. Venables, J. A. Atomic processes in crystal-growth. *Surf. Sci.* **299**, 798–817 (1994).
16. Liu, Y. H. et al. Deposition of multicomponent metallic glass films by single-target magnetron sputtering. *Intermetallics* **21**, 105–114 (2012).
17. Ohring M. *Materials Science of Thin Films: Deposition and Structure*, 2nd edn. (Academic Press, 2002).
18. Fakhraai, Z. & Forrest, J. A. Measuring the surface dynamics of glassy polymers. *Science* **319**, 600–604 (2008).
19. Sun, G., Saw, S., Douglass, I. & Harrowell, P. Structural origin of enhanced dynamics at the surface of a glassy alloy. *Phys. Rev. Lett.* **119**, 245501 (2017).
20. Cao, C. R. et al. Liquid-like behaviours of metallic glassy nanoparticles at room temperature. *Nat. Commun.* **10**, 1966 (2019).
21. Tian, Y. et al. Fast coalescence of metallic glass nanoparticles. *Nat. Commun.* **10**, 5249 (2019).
22. Chen, N. et al. Direct observation of fast surface dynamics in sub-10-nm nanoglass particles. *Appl. Phys. Lett.* **114**, 043103 (2019).
23. Chai, Y. et al. A direct quantitative measure of surface mobility in a glassy polymer. *Science* **343**, 994–999 (2014).
24. Yuan, C. C. & Xi, X. K. On the correlation of Young's modulus and the fracture strength of metallic glasses. *J. Appl. Phys.* **109**, 033515 (2011).
25. Lagogianni, A. E., Papageorgiou, D. G. & Evangelakis, G. A. Surface properties of the Cu50Zr50 metallic glass decorated with icosahedral CuxZr100-x (0 < x < 100) clusters by molecular dynamics simulations. *Comp. Mater. Sci.* **54**, 145–149 (2012).
26. Jiang, Q. K. et al. Zr-(Cu,Ag)-Al bulk metallic glasses. *Acta Mater.* **56**, 1785–1796 (2008).
27. Yu, H. B., Wang, W. H. & Bai, H. Y. An electronic structure perspective on glass-forming ability in metallic glasses. *Appl. Phys. Lett.* **96**, 081902 (2010).
28. Jeffers, G., Dubson, M. A. & Duxbury, P. M. Island-to-percolation transition during growth of metal-films. *J. Appl. Phys.* **75**, 5016–5020 (1994).
29. Zhang, Y., Mattern, N. & Eckert, J. Understanding the relationship between atomic structures and transport properties in (Cu0.5Zr0.5)(100-x)Al-x (<= 10) glass forming liquids: molecular dynamics simulations. *J. Alloy Compd.* **514**, 141–149 (2012).
30. Cao, C. R., Lu, Y. M., Bai, H. Y. & Wang, W. H. High surface mobility and fast surface enhanced crystallization of metallic glass. *Appl. Phys. Lett.* **107**, 141606 (2015).
31. Zhu, L. et al. Surface self-diffusion of an organic glass. *Phys. Rev. Lett.* **106**, 256103 (2011).
32. Malshe, R., Ediger, M. D., Yu, L. & de Pablo, J. J. Evolution of glassy gratings with variable aspect ratios under surface diffusion. *J. Chem. Phys.* **134**, 194704 (2011).
33. Zhang, Y. & Fakhraai, Z. Invariant fast diffusion on the surfaces of ultrastable and aged molecular glasses. *Phys. Rev. Lett.* **118**, 066101 (2017).
34. Ruan S., Zhang W., Sun Y., Ediger M. D., Yu L. Surface diffusion and surface crystal growth of tris-naphthyl benzene glasses. *J. Chem. Phys.* **145**, 064503 (2016).
35. Chen, H., Qu, B. Y., Li, D. D., Zhou, R. L. & Zhang, B. Atomic structure and dynamics properties of Cu50Zr50 films. *J. Appl. Phys.* **123**, 025307 (2018).
36. Luttich, M. et al. Anti-aging in ultrastable metallic glasses. *Phys. Rev. Lett.* **120**, 135504 (2018).
37. Dawson, K. J., Zhu, L., Yu, L. A. & Ediger, M. D. Anisotropic structure and transformation kinetics of vapor-deposited indomethacin glasses. *J. Phys. Chem. B* **115**, 455–463 (2011).

Acknowledgements

Author contributions

Y.L. conceived and supervised the research. F.Y. and Y.L. designed the experiments. F.Y. performed the experiments. F.Y. and Y.L. analyzed the data. All authors discussed the data. F.Y. and Y.L. wrote the manuscript with contributions from C.W., H.B. and W.H.

Competing interests

The authors declare no competing interests.

Additional information

Supplementary information The online version contains supplementary material available at https://doi.org/10.1038/s43246-021-00180-9.

Correspondence and requests for materials should be addressed to Y.L.

Peer review information Communications Materials thanks the anonymous reviewers for their contribution to the peer review of this work. Primary Handling Editors: John Plummer.

Reprints and permission information is available at http://www.nature.com/reprints

Publisher's note Springer Nature remains neutral with regard to jurisdictional claims in published maps and institutional affiliations.